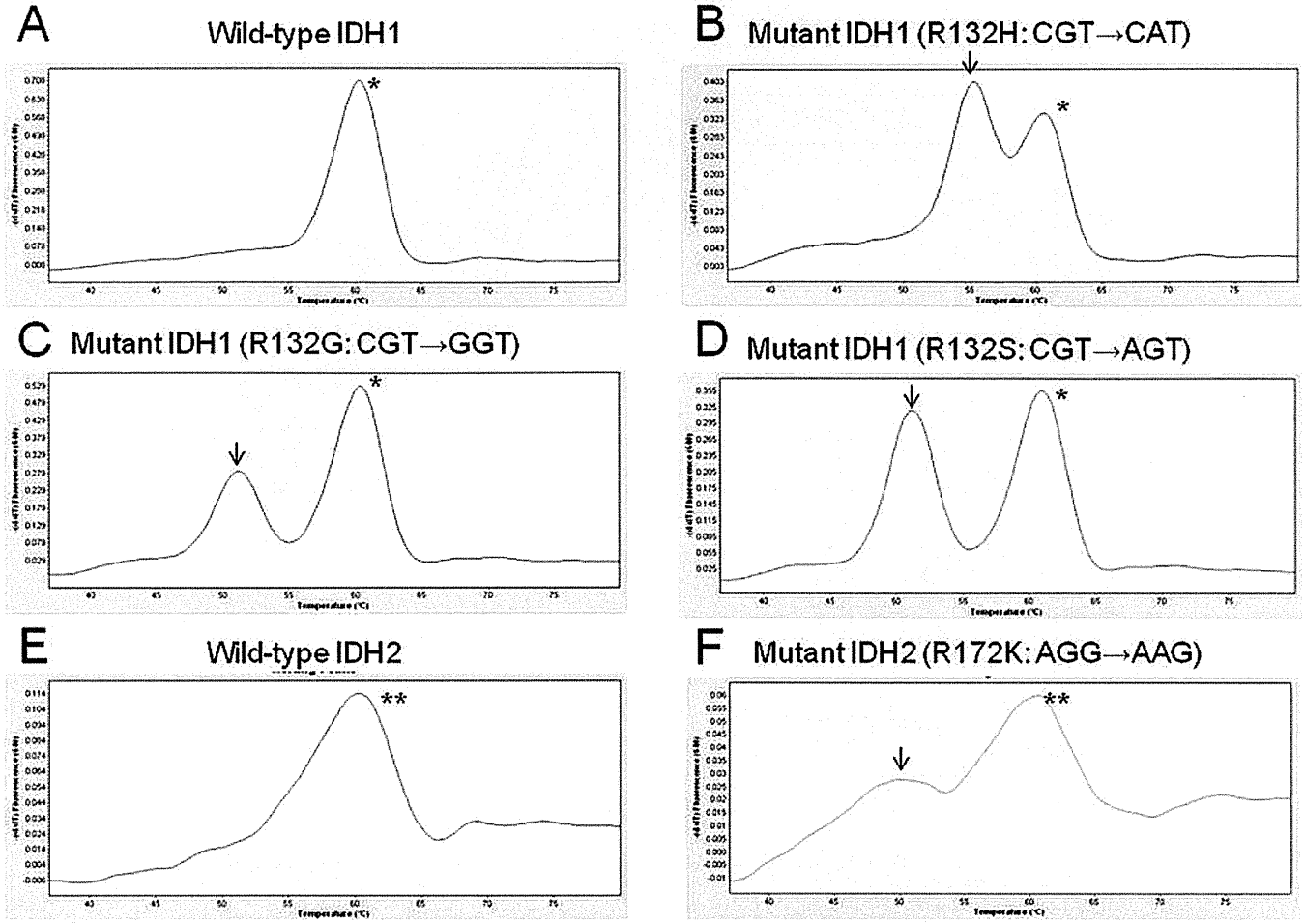

FIG. 1. Fluorescent curve analysis of conventional PCR fragments of *IDH1* and *IDH2* genes from rapidly extracted DNA for intraoperative detection. **A–D:** Fluorescent melting curve analysis of PCR fragments, including the site of *IDH1* gene mutation. All types of mutation (CAT, GGT, and AGT) had a distinct Tm *(arrows)* from the wild-type sequence *(single asterisk)*. **E and F:** Fluorescent melting curve analysis of PCR fragments, including the site of *IDH2* gene mutations. Mutation of the *IDH2* gene had a distinct Tm *(arrow)* from the wild-type sequence *(double asterisks)*.

in 3 cases (Cases 2, 3, and 5 in Table 1; Figs. 3 and 4), whereas no *IDH1* and *IDH2* gene mutation was found in 2 cases (Cases 1 and 4). H & E staining of formalin-fixed, paraffin-embedded sections established diagnoses of diffuse astrocytoma in 2, oligodendroglioma in 2, and oligoastrocytoma in 1 case. Case 5 had a diffuse lesion in the left temporal lobe (Fig. 4A). The finding of cells with low-grade atypia distributed unevenly with low cellularity on intraoperative frozen sections is indicative of low-grade glioma (Fig. 4B). Conventional PCR and FMCA with HybProbe detected a slight peak other than that of wild-type allele, and COLD-PCR enriched the mutant sequence (Fig. 4C). Immunohistochemical analysis of the specimen from this lesion revealed that one-third of cells expressed mutant IDH1 protein (Fig. 4D).

Detection of IDH1 *and* IDH2 *Mutations in High-Grade Glioma*

During the cohort period, 10 cases of high-grade glioma were suspected based on MRI. The diagnoses based on frozen sections and formalin-fixed, paraffin-embedded sections, as well as the mutation status, are shown in Table 1 (Cases 9–18). Intraoperative frozen-section examination suggested diagnoses of glioblastoma in 5 cases. Intraoperative detection of the *IDH1* or *IDH2* gene revealed no mutation in 4 of these cases and an *IDH1* gene mutation in 1 of the cases. The final histological diagnoses of the cases without mutation were glioblastoma in 3 and glioblastoma with an oligodendroglial component in 1, and the diagnosis of the case with mutation was glioblastoma. Another 5 cases were diagnosed as high-grade glioma without evidence of glioblastoma. Intraoperative diagnosis based on frozen sections was anaplastic astrocytoma in 2 and anaplastic oligodendroglioma in 3. We detected the *IDH1* gene mutation in 3 cases, and final histological diagnosis of these cases was anaplastic oligodendroglioma.

Differentiation of Recurrence From Treatment-Induced Changes

To examine whether our procedures could detect the presence of tumor cells in radiation necrosis, we evaluated the frozen tissues and formalin-fixed, paraffin-embedded

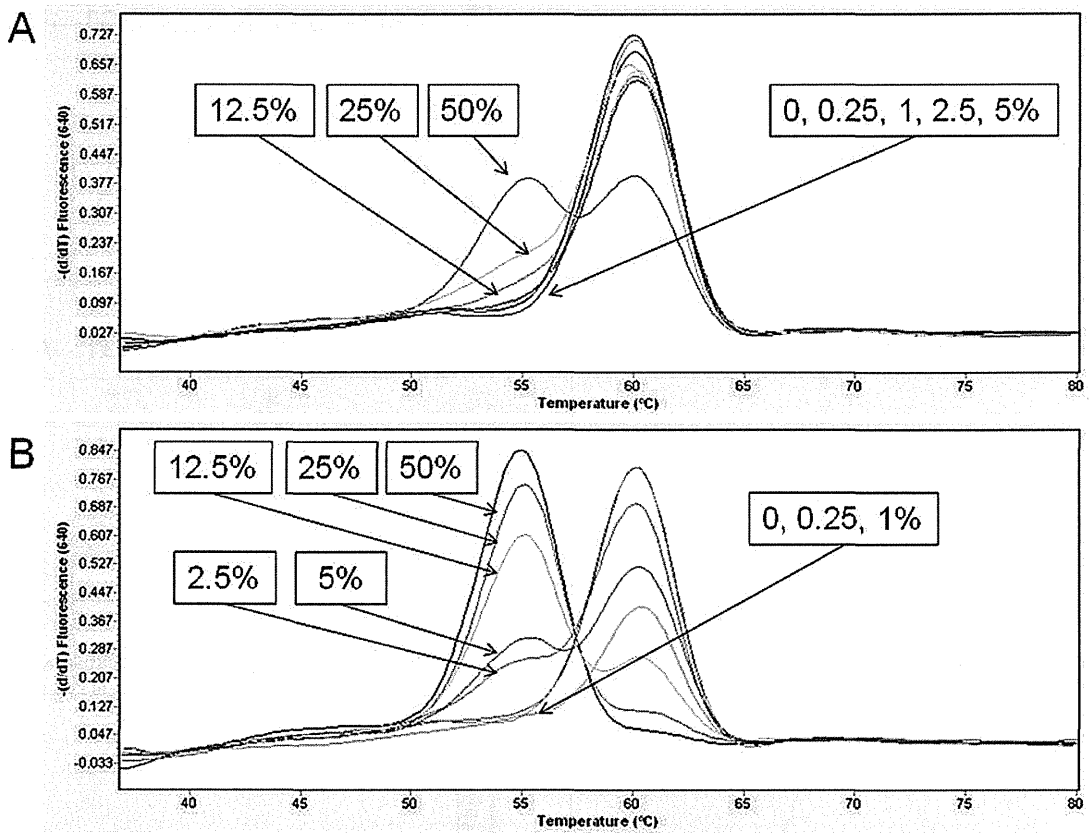

FIG. 2. Fluorescent melting curve analysis after conventional PCR (**A**) and co-amplification at lower denaturation temperature (COLD-PCR; **B**) for the detection of *IDH1* R132H mutation. Mutant DNA from tumors with *IDH1* R132H mutation was serially diluted with wild-type DNA from tumor without *IDH1* mutation.

sections from 3 specimens of radiation necrosis containing a small fraction of reactive astrocytes or tumor cells. Conventional PCR and FMCA with HybProbe detected low signals corresponding to the mutated sequence in all 3 cases, and the mutated sequence could be enriched with COLD-PCR in all 3 cases (Fig. 5A). We confirmed this finding with immunohistochemistry for mutated IDH1 protein, and found a small fraction of cells expressing mutated IDH1 protein within the necrotic tissue in all 3 cases (Fig. 5B and C).

Discussion

In the present study we investigated intraoperative procedures for the detection of mutations in the *IDH1* and *IDH2* genes. Various methods are available for their detection, with the greatest sensitivity being high as 0.0002% when using COLD-PCR followed by targeted resequencing,[15] and the fastest method for amplification and detection being FMCA, which can detect mutation in 80 minutes using extracted DNA.[8] Our present method detected mutation in 60–65 minutes from sampling of specimens to extraction of DNA and detected *IDH1* mutation as low as 2.5% against a background of the wild-type allele. This study showed that our simple method was feasible for the intraoperative detection of mutation and demonstrated complete concordance with the results obtained from standard DNA extraction and Sanger sequencing.

The most important application for intraoperative molecular diagnosis is providing definitive, objective, and rapid information to guide the surgical procedures. We found that FMCA with one pair of specific probes for the mutational hotspot[8] could provide exact information on the mutation status, heterozygosity, and proportions of mutant alleles in the tissue examined. In addition, we employed COLD-PCR as well as conventional PCR. COLD-PCR was highly sensitive for detection of the low abundance of mutated alleles in Case 5 and in cases of radiation necrosis with a small fraction of tumor cells carrying the *IDH1* gene mutation. In addition, this PCR-based detection system requires small samples obtained by 2-mm tumor forceps. Procedures for intraoperative diagnosis require rapidity. We achieved detection of mutation within 60–65 minutes. Double COLD-PCR has been followed by high-resolution melting analysis with an 0.25% sensitivity for detection of mutant allele.[2] The extraction of DNA using the QIAamp DNA extraction kit, according to the manufacturer's instructions, took 90–270 minutes, and amplification of the DNA fragment and detection of the mutation took 180 minutes.[3] Such a method is clearly applicable to postoperative meticulous study, but this method seems to be too sensitive and takes too much time for the intraoperative qualitative diagnosis of glioma. Although

TABLE 1: Results of rapid detection of *IDH1* and *IDH2* mutations and diagnosis based on examination of intraoperative frozen sections and paraffin-embedded sections*

Case No.	Age (yrs), Sex	Diagnosis		*IDH1* Status		*IDH2* Status:
		Using Frozen Sections	Using FFPE Sections	PCR	COLD-PCR	PCR
1	18, F	nonneoplastic tissue or LGG	diffuse astrocytoma	wt	wt	wt
2	41, F	nonneoplastic tissue or LGG	oligodendroglioma	mut	ND	ND
3	22, F	nonneoplastic tissue or LGG	diffuse astrocytoma	mut	ND	ND
4	77, M	nonneoplastic tissue or LGG	oligodendroglioma	wt	wt	wt
5	63, F	nonneoplastic tissue or LGG	oligoastrocytoma	mut†	mut	wt
6	31, F	oligoastrocytoma	oligoastrocytoma	mut	ND	ND
7	49, F	oligodendroglioma	oligodendroglioma	mut	ND	ND
8	25, F	ganglioglioma	anaplastic ganglioglioma	mut	ND	wt
9	48, M	anaplastic astrocytoma	GBMO	wt	wt	wt
10	38, F	anaplastic astrocytoma	anaplastic oligodendroglioma	mut	ND	wt
11	52, M	anaplastic oligodendroglioma	anaplastic oligodendroglioma	mut	ND	wt
12	47, F	anaplastic oligodendroglioma	anaplastic oligodendroglioma	mut	ND	wt
13	56, M	anaplastic oligodendroglioma	GBMO	wt	wt	wt
14	52, M	glioblastoma	glioblastoma	wt	wt	wt
15	60, M	glioblastoma	GBMO	wt	wt	wt
16	42, M	glioblastoma	glioblastoma	mut	ND	wt
17	59, M	glioblastoma	glioblastoma	wt	wt	wt
18	62, F	glioblastoma	glioblastoma	wt	wt	wt

* FFPE = formalin-fixed, paraffin-embedded; GBMO = glioblastoma with oligodendroglioma component; LGG = low-grade glioma; mut = mutant; ND = not done; wt = wild-type.

† Low peak of mutated sequence.

we achieved intraoperative detection of the mutation within 60–65 minutes, further shortening of the assay time would increase the applicability of the method. We could shorten the time for DNA extraction (from 90 to 270 minutes to 15 minutes) and for detection of the mutation (from 180 minutes with Sanger sequencing to 5 minutes). The time for DNA amplification took 40–45 minutes, and simpler technology could further reduce the time required. For example, loop-mediated isothermal amplification is a novel nucleic acid amplification method that amplifies DNA with high specificity, efficiency, and rapidity.[17] This method requires a set of 4 specially designed primers and a DNA polymerase with strand displacement activity under isothermal conditions, needs only 15 minutes to amplify the DNA,[28] and has been applied to the detection of microbial diseases and metastatic cancer cells.[10,19]

The quality of any clinical test depends on its validity and predictive value. Validity and predictive value consist of sensitivity and specificity and positive and negative predictive values, respectively. To assess the validity and predictive values, we have to discuss the 2 objectives of this test: 1) intraoperative detection of mutation of *IDH* genes and 2) detection of the "glioma." If the detection of the *IDH* mutation is the main goal, the sensitivity/specificity and the positive and negative predictive values are all 100%, as no false-positive or -negative results were found in the 14 cases of the validation study and the 18 cases of the intraoperative study. These parameters may be superior to those of Sanger sequencing, in which the detection threshold was 25% (data not shown) of the *IDH1* mutation against a background of the wild-type allele, and immunohistochemistry for R132H IDH1 mutation, in which any other type of mutation of *IDH1* or *IDH2* could not be detected. However, we need to be cautious in interpreting this result. The threshold for detection was 2.5% of the *IDH1* mutation against a background of the wild-type allele, whereas an insufficient sampling with a low tumor/normal cell ratio decreased the sensitivity and negative predictive value. If detection of the "glioma" is the main objective, then the sensitivity and specificity are very different. In this series, the sensitivity for the detection of glioma was 44%. Since the mutations of *IDH1* and *IDH2* are high-abundance mutations in gliomas, this result depends on the frequency of the cases with *IDH* mutation established by adequate sampling. Specificity could not be assessed because no cases of nonneoplastic lesions were included in the study. However, high specificity can be expected because previous reports suggested that no nonneoplastic lesions had *IDH1* and *IDH2* mutations.[3,9]

With regard to predictive value, the intraoperative detection of mutation had a 100% positive predictive value for glioma. This is the most important clinical aspect to apply in intraoperative genetic diagnosis. If intraoperative diagnosis based on morphology cannot establish the definitive diagnosis as glioma, the surgeon has to discontinue the surgery and to await the results of histological diagnosis. However, the detection of an *IDH1* or *IDH2* mutation definitively indicates that the lesion contains

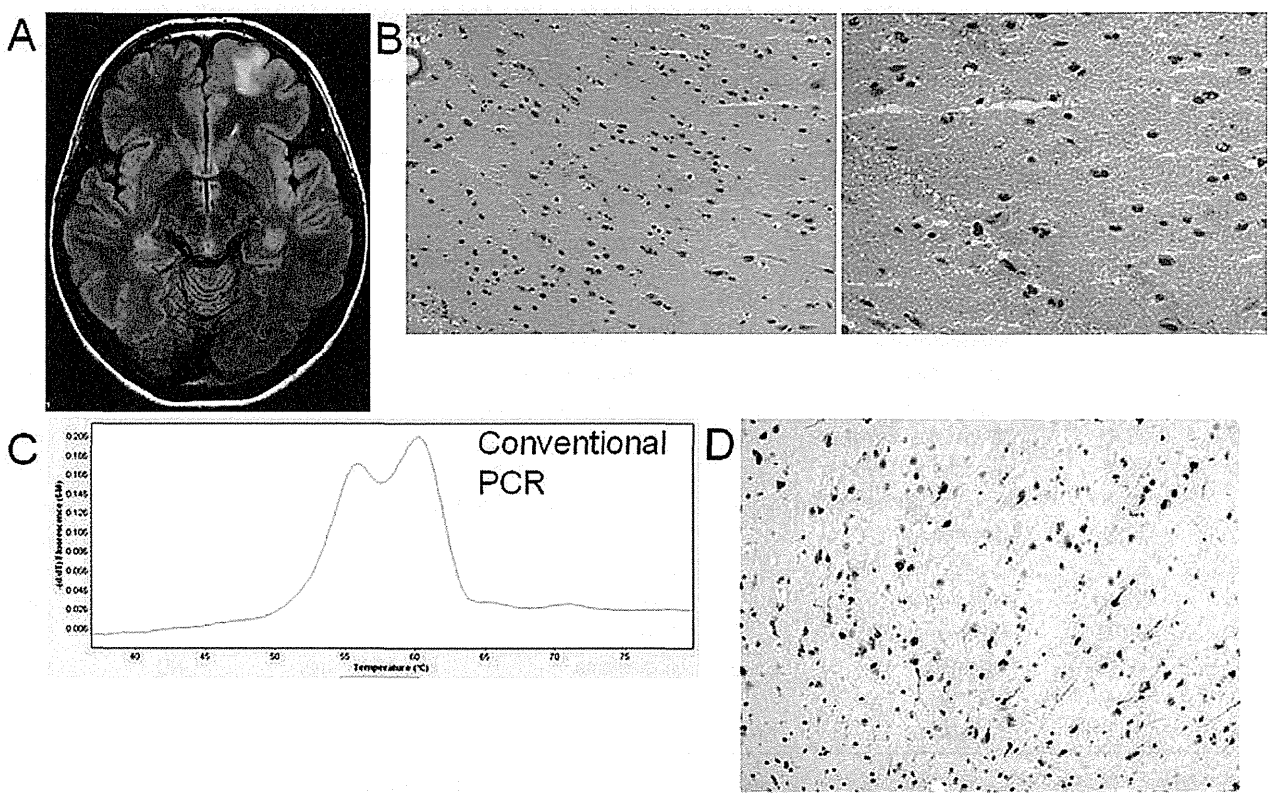

FIG. 3. Case 3. Representative case of a 22-year-old woman with an asymptomatic diffuse lesion in the left frontal lobe. **A:** Preoperative FLAIR MR image demonstrating the diffuse lesion in the left frontal lobe. **B:** H & E staining of the intraoperative frozen section demonstrating cells with slight nuclear atypia distributed unevenly with low cellularity; however, these changes were not conclusive of a diagnosis for low-grade glioma. Original magnification ×200 *(left)* and ×400 *(right)*. **C:** Fluorescent melting curve analysis after conventional PCR for the detection of the *IDH1* mutation, demonstrating tissues containing the wild-type and mutant *IDH1* gene. **D:** Immunohistochemistry for mutant IDH1 R132H protein of a formalin-fixed, paraffin-embedded section from the same region, demonstrating that tumor cells express mutant IDH1 R132H protein. Original magnification ×200.

glioma. Therefore, an intraoperative molecular diagnosis could provide critical information during surgery for tumors suspected to be low-grade glioma. In contrast, 2 of 5 cases in which a nonneoplastic lesion was difficult to differentiate from low-grade glioma had wild-type *IDH1* and *IDH2* genes. Because the absence of an *IDH* mutation does not imply that the lesion is a nonneoplastic lesion, the negative predictive value for glioma was unsatisfactory based only on *IDH1* and *IDH2* gene analysis. Similarly, 6 of 10 cases with high-grade glioma had wild-type *IDH1* and *IDH2* genes. To improve the negative predictive value of intraoperative molecular diagnosis in the future, multiplex analysis with mutation sets for detecting glioma is desirable. To date, the specific mutations such as the *BRAF* V600E mutation in pleomorphic xanthoastrocytoma, ganglioglioma, and pediatric astrocytoma[23,24] and the histone H3.3 K27 M mutation in diffuse intrinsic pontine glioma[31] have been reported, and they are potential candidates for intraoperative molecular analysis. Further comprehensive sequence analysis of various types of tumors and nonneoplastic lesions with the next generation of sequencer technology may achieve high negative predictive value for clinical use, and detection of other disease- or tumor-specific mutations may encourage wider use of intraoperative detection systems in the future.

The expected implication of intraoperative diagnosis is that the neurosurgeon can decide the extent of resection based on the mutation status. We found this method useful for the differential diagnosis of anaplastic oligodendroglial tumors, glioblastoma with an oligodendroglioma component, and glioblastoma, as demonstrated in Cases 11, 12, 13, and 15, based on the diverse frequency of the *IDH1* or *IDH2* gene.[1,7,30] As these entities have quite different prognoses,[16] this method is valuable for establishing the prognosis of the case intraoperatively. However, this intraoperative examination is no more than a diagnostic technique of mutation status and histological subtypes and is not useful for deciding the extent of resection. To this end, the differences in the sensitivity to adjuvant radiation therapy/chemotherapy and in the impact of the extent of the resection between glioma with mutated and wild-type *IDH1* genes should be elucidated. To our knowledge, 3 previously reported studies have demonstrated differences in the sensitivity to adjuvant therapy in tumors with mutated and wild-type *IDH1* genes. A hazards ratio reduction by the addition of chemotherapy (procarbazine, CCNU, and vincristine) was more pronounced in patients with anaplastic oligodendroglial tumors with *IDH1* mutation.[29] Similarly, the presence of an *IDH* mutation predicts response to temozolomide in

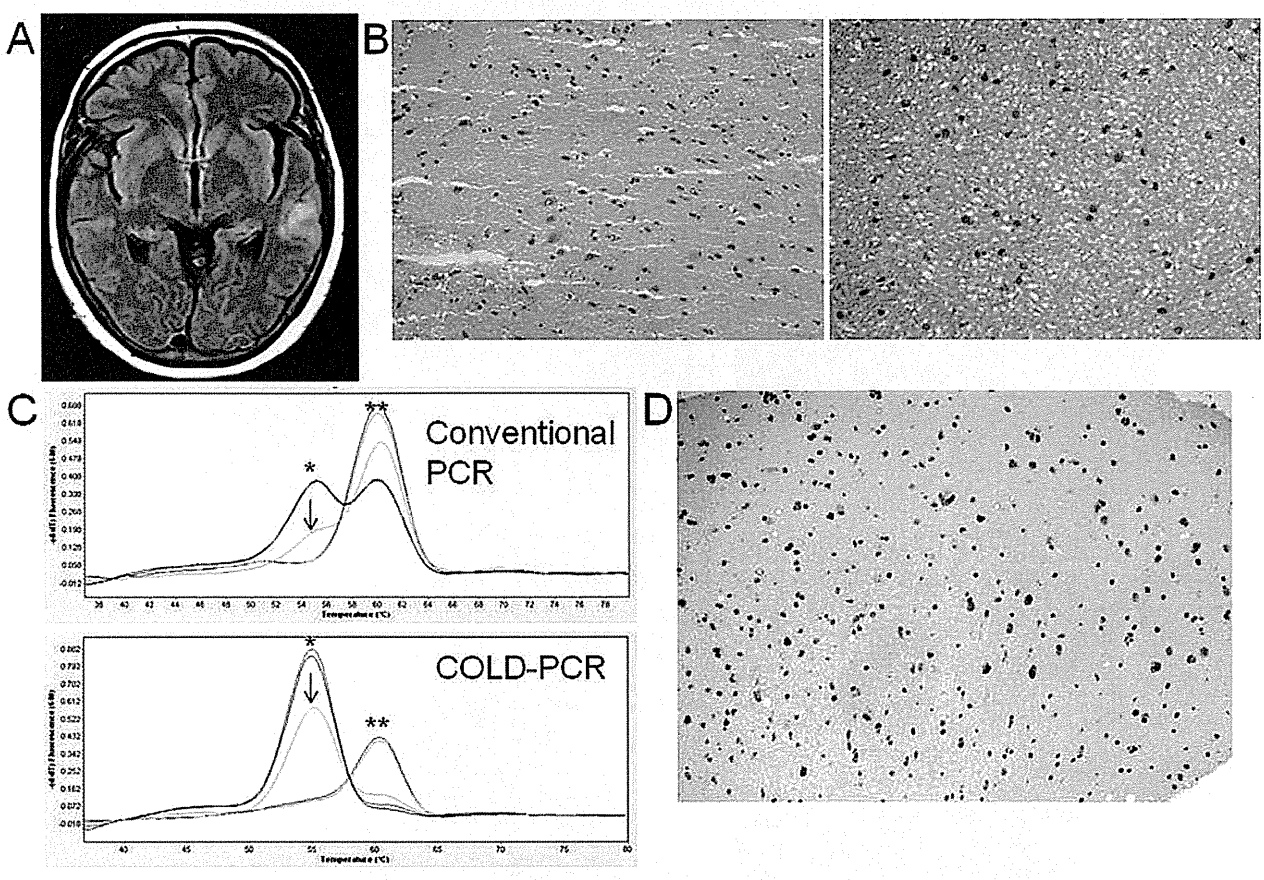

FIG. 4. Case 5. Representative case of a 63-year-old woman with an asymptomatic diffuse lesion in the left temporal lobe. **A:** Preoperative FLAIR MR image demonstrating the diffuse lesion in the left temporal lobe. **B:** H & E staining of the intraoperative frozen section demonstrating uneven distribution of cells with slight nuclear atypia with low cellularity; however, these changes were not conclusive of a diagnosis of low-grade glioma. Original magnification ×200 *(left)* and ×400 *(right)*. **C:** Fluorescent melting curve analysis after conventional PCR *(upper)* and co-amplification at lower denaturation temperature (COLD-PCR; *lower*), demonstrating a low peak of the mutation *(arrow)* after conventional PCR, and a clearer peak of the mutation *(arrow)* after COLD-PCR. Same analysis of DNA from the tumor carrying mutated *(asterisk)* and wild-type *(double asterisks) IDH1* gene was used as the control. **D:** Immunohistochemistry for mutant IDH1 R132H protein of a formalin-fixed, paraffin-embedded section from the same region, demonstrating that one-third of the cells expressed mutant IDH1 R132H protein. Original magnification ×200.

low-grade gliomas and secondary glioblastomas.[11,26] In contrast, little reliable information is available to demonstrate any difference in the impact of the extent of resection in glioma with a mutated and wild-type *IDH1/IDH2* gene. If any difference between glioma with mutated or wild-type *IDH* genes can be demonstrated in the future, an intraoperative molecular diagnosis will provide useful information for designing the surgical strategy.

In the present study, using intraoperative frozen-tissue examination, we detected an *IDH1* mutation in all 3 cases that involved a diagnosis of radiation necrosis with a small fraction of tumor cells. A previous report provided objective evidence for the presence of glioma cells in most cases of radiation necrosis and without definitive tumor demonstrated on H & E–stained photomicrographs.[3] Mutant IDH1 protein was consistently detected in posttherapy glioma with mutation of *IDH1* at first biopsy.[3] Considered together with our results, the observation that posttherapy glioma tissues always contain glioma cells indicates that it is meaningless to apply this technology for only intraoperative detection of tumor cells during the surgery for recurrent glioma. Instead, we can estimate the proportion of tumor cells to normal cells with the PCR and COLD-PCR methods as shown in Fig. 2. For clinical application in the surgery of recurrent glioma, it might be useful to examine the correlation between the proportion of mutated alleles and prognosis, combined with intraoperative assessment of proliferative activity shown using Ki-67 immunostaining.[6]

Conclusions

The combination of rapid extraction of DNA and conventional PCR, followed by FMCA with HybProbe, provides a quick and specific method for intraoperative detection of *IDH1* and *IDH2* gene mutations. COLD-PCR enhanced the sensitivity for detection of the *IDH1* gene mutation and is applicable to intraoperative molecular diagnosis. These methods were useful in the differential diagnosis between low-grade glioma and nonneo-

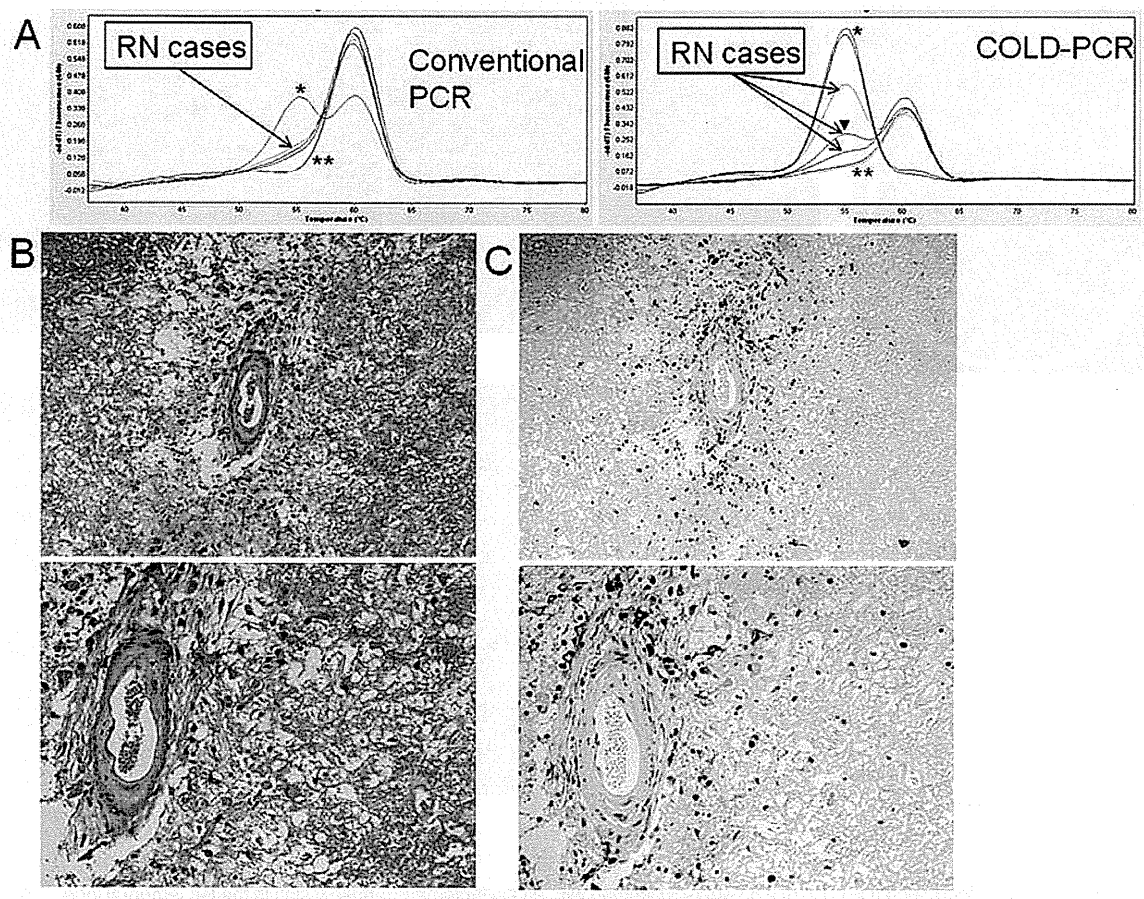

FIG. 5. Simulated detection of mutation from the tissue with radiation necrosis (RN). **A:** Fluorescent melting curve analysis after conventional PCR and co-amplification at lower denaturation temperature (COLD-PCR) for the detection of *IDH1* mutation in the frozen tissues, obtained from 3 cases diagnosed with radiation necrosis on formalin-fixed, paraffin-embedded sections (indicated as RN cases), demonstrating the presence of the mutation in all 3 cases. Note that COLD-PCR enhanced the sensitivity for detection. The same analysis of DNA from the tumor with mutated *(single asterisk)* and wild-type *(double asterisks) IDH1* genes was used as the control. **B and C:** H & E staining (B) and immunohistochemistry for mutant IDH1 R132H protein (C) of a formalin-fixed, paraffin-embedded section of the representative case with radiation necrosis, demonstrating gemistocytic cells around the vessel in the background of necrotic tissue, and several gemistocytic cells expressing mutant IDH1 R132H protein around the vessel. Original magnification ×100 (B upper and C upper) and ×400 (B lower and C lower).

plastic lesions, the diagnosis for subtypes of high-grade glioma, and the prediction of the prognosis. Although tumor cells in cases of radiation necrosis were detected with high sensitivity, further investigation is necessary to establish clinical application.

Acknowledgment

We thank Ms. Misaki Fue for her technical assistance in the intraoperative assays.

Disclosure

The authors report no conflict of interest concerning the materials or methods used in this study or the findings specified in this paper.

Author contributions to the study and manuscript preparation include the following. Conception and design: Kanamori, Kikuchi, Kumabe, Tominaga. Acquisition of data: Kanamori, Kikuchi, Watanabe, Shibahara, Saito, Yamashita, Sonoda, Kumabe. Analysis and interpretation of data: Kanamori, Saito, Yamashita, Kure. Drafting the article: Kanamori, Kikuchi, Watanabe, Kure, Tominaga. Critically revising the article: all authors. Reviewed submitted version of manuscript: all authors. Approved the final version of the manuscript on behalf of all authors: Kanamori. Administrative/technical/material support: Kanamori. Study supervision: Kanamori, Tominaga.

References

1. Balss J, Meyer J, Mueller W, Korshunov A, Hartmann C, von Deimling A: Analysis of the IDH1 codon 132 mutation in brain tumors. **Acta Neuropathol 116:**597–602, 2008
2. Boisselier B, Marie Y, Labussière M, Ciccarino P, Desestret V, Wang X, et al: COLD PCR HRM: a highly sensitive detection method for IDH1 mutations. **Hum Mutat 31:**1360–1365, 2010
3. Capper D, Sahm F, Hartmann C, Meyermann R, von Deimling A, Schittenhelm J: Application of mutant IDH1 antibody to differentiate diffuse glioma from nonneoplastic central nervous system lesions and therapy-induced changes. **Am J Surg Pathol 34:**1199–1204, 2010
4. Capper D, Zentgraf H, Balss J, Hartmann C, von Deimling A: Monoclonal antibody specific for IDH1 R132H mutation. **Acta Neuropathol 118:**599–601, 2009

5. Felsberg J, Wolter M, Seul H, Friedensdorf B, Göppert M, Sabel MC, et al: Rapid and sensitive assessment of the IDH1 and IDH2 mutation status in cerebral gliomas based on DNA pyrosequencing. **Acta Neuropathol 119:**501–507, 2010
6. Haapasalo J, Mennander A, Helen P, Haapasalo H, Isola J: Ultrarapid Ki-67 immunostaining in frozen section interpretation of gliomas. **J Clin Pathol 58:**263–268, 2005
7. Hegi ME, Janzer RC, Lambiv WL, Gorlia T, Kouwenhoven MC, Hartmann C, et al: Presence of an oligodendroglioma-like component in newly diagnosed glioblastoma identifies a pathogenetically heterogeneous subgroup and lacks prognostic value: central pathology review of the EORTC_26981/NCIC_CE.3 trial. **Acta Neuropathol 123:**841–852, 2012
8. Horbinski C, Kelly L, Nikiforov YE, Durso MB, Nikiforova MN: Detection of IDH1 and IDH2 mutations by fluorescence melting curve analysis as a diagnostic tool for brain biopsies. **J Mol Diagn 12:**487–492, 2010
9. Horbinski C, Kofler J, Kelly LM, Murdoch GH, Nikiforova MN: Diagnostic use of IDH1/2 mutation analysis in routine clinical testing of formalin-fixed, paraffin-embedded glioma tissues. **J Neuropathol Exp Neurol 68:**1319–1325, 2009
10. Horibe D, Ochiai T, Shimada H, Tomonaga T, Nomura F, Gun M, et al: Rapid detection of metastasis of gastric cancer using reverse transcription loop-mediated isothermal amplification. **Int J Cancer 120:**1063–1069, 2007
11. Houillier C, Wang X, Kaloshi G, Mokhtari K, Guillevin R, Laffaire J, et al: IDH1 or IDH2 mutations predict longer survival and response to temozolomide in low-grade gliomas. **Neurology 75:**1560–1566, 2010
12. Kanamori M, Kumabe T, Shibahara I, Saito R, Yamashita Y, Sonoda Y, et al: Clinical and histological characteristics of recurrent oligodendroglial tumors: comparison between primary and recurrent tumors in 18 cases. **Brain Tumor Pathol 30:**151–159, 2013
13. Li J, Wang L, Mamon H, Kulke MH, Berbeco R, Makrigiorgos GM: Replacing PCR with COLD-PCR enriches variant DNA sequences and redefines the sensitivity of genetic testing. **Nat Med 14:**579–584, 2008
14. Louis DN, Ohgaki H, Wiestler OD, Cavenee WK: **WHO Classification of Tumours of the Central Nervous System.** Lyon: IARC Press, 2007
15. Milbury CA, Correll M, Quackenbush J, Rubio R, Makrigiorgos GM: COLD-PCR enrichment of rare cancer mutations prior to targeted amplicon resequencing. **Clin Chem 58:**580–589, 2012
16. Miller CR, Dunham CP, Scheithauer BW, Perry A: Significance of necrosis in grading of oligodendroglial neoplasms: a clinicopathologic and genetic study of newly diagnosed high-grade gliomas. **J Clin Oncol 24:**5419–5426, 2006
17. Notomi T, Okayama H, Masubuchi H, Yonekawa T, Watanabe K, Amino N, et al: Loop-mediated isothermal amplification of DNA. **Nucleic Acids Res 28:**E63, 2000
18. Ohgaki H, Kleihues P: The definition of primary and secondary glioblastoma. **Clin Cancer Res 19:**764–772, 2013
19. Parida M, Sannarangaiah S, Dash PK, Rao PV, Morita K: Loop mediated isothermal amplification (LAMP): a new generation of innovative gene amplification technique; perspectives in clinical diagnosis of infectious diseases. **Rev Med Virol 18:**407–421, 2008
20. Parsons DW, Jones S, Zhang X, Lin JC, Leary RJ, Angenendt P, et al: An integrated genomic analysis of human glioblastoma multiforme. **Science 321:**1807–1812, 2008
21. Plesec TP, Prayson RA: Frozen section discrepancy in the evaluation of central nervous system tumors. **Arch Pathol Lab Med 131:**1532–1540, 2007
22. Roessler K, Dietrich W, Kitz K: High diagnostic accuracy of cytologic smears of central nervous system tumors. A 15-year experience based on 4,172 patients. **Acta Cytol 46:**667–674, 2002
23. Schiffman JD, Hodgson JG, VandenBerg SR, Flaherty P, Polley MY, Yu M, et al: Oncogenic BRAF mutation with CDKN2A inactivation is characteristic of a subset of pediatric malignant astrocytomas. **Cancer Res 70:**512–519, 2010
24. Schindler G, Capper D, Meyer J, Janzarik W, Omran H, Herold-Mende C, et al: Analysis of BRAF V600E mutation in 1,320 nervous system tumors reveals high mutation frequencies in pleomorphic xanthoastrocytoma, ganglioglioma and extra-cerebellar pilocytic astrocytoma. **Acta Neuropathol 121:**397–405, 2011
25. Shibahara I, Sonoda Y, Kanamori M, Saito R, Yamashita Y, Kumabe T, et al: IDH1/2 gene status defines the prognosis and molecular profiles in patients with grade III gliomas. **Int J Clin Oncol 17:**551–561, 2012
26. SongTao Q, Lei Y, Si G, YanQing D, HuiXia H, XueLin Z, et al: IDH mutations predict longer survival and response to temozolomide in secondary glioblastoma. **Cancer Sci 103:** 269–273, 2012
27. Sonoda Y, Kumabe T, Nakamura T, Saito R, Kanamori M, Yamashita Y, et al: Analysis of IDH1 and IDH2 mutations in Japanese glioma patients. **Cancer Sci 100:**1996–1998, 2009
28. Tsujimoto M, Nakabayashi K, Yoshidome K, Kaneko T, Iwase T, Akiyama F, et al: One-step nucleic acid amplification for intraoperative detection of lymph node metastasis in breast cancer patients. **Clin Cancer Res 13:**4807–4816, 2007
29. van den Bent MJ, Brandes AA, Taphoorn MJ, Kros JM, Kouwenhoven MC, Delattre JY, et al: Adjuvant procarbazine, lomustine, and vincristine chemotherapy in newly diagnosed anaplastic oligodendroglioma: long-term follow-up of EORTC brain tumor group study 26951. **J Clin Oncol 31:**344–350, 2013
30. Wang Y, Li S, Chen L, You G, Bao Z, Yan W, et al: Glioblastoma with an oligodendroglioma component: distinct clinical behavior, genetic alterations, and outcome. **Neuro Oncol 14:**518–525, 2012
31. Wu G, Broniscer A, McEachron TA, Lu C, Paugh BS, Becksfort J, et al: Somatic histone H3 alterations in pediatric diffuse intrinsic pontine gliomas and non-brainstem glioblastomas. **Nat Genet 44:**251–253, 2012

Manuscript submitted July 14, 2013.
Accepted March 13, 2014.
Please include this information when citing this paper: published online April 18, 2014; DOI: 10.3171/2014.3.JNS131505.

Address correspondence to: Masayuki Kanamori, M.D., Ph.D., Department of Neurosurgery, Tohoku University Graduate School of Medicine, 1-1 Seiryo-machi, Aoba-ku, Sendai, Miyagi 980-8574, Japan. email: mkanamori@med.tohoku.ac.jp.

Neuro-Oncology Advance Access published March 3, 2013
Neuro-Oncology
doi:10.1093/neuonc/not020
NEURO-ONCOLOGY

Bevacizumab treatment of symptomatic pseudoprogression after boron neutron capture therapy for recurrent malignant gliomas. Report of 2 cases

Shin-Ichi Miyatake, Motomasa Furuse, Shinji Kawabata, Takashi Maruyama, Toshihiro Kumabe, Toshihiko Kuroiwa, and Koji Ono

Department of Neurosurgery, Osaka Medical College, Takatsuki, Osaka, Japan (S.-I.M., M.F., S.K., T.K.); Department of Neurosurgery, Tokyo Women's Medical College, Shinjuku, Tokyo, Japan (T.M.); Department of Neurosurgery, Tohoku University, Sendai, Miyagi, Japan (T.K.); Radiation Oncology and Particle Radiation Oncology Research Center, Research Reactor Institute, Kyoto University, Kumatori, Osaka, Japan (K.O.)

Background. Bevacizumab, an anti–vascular endothelial growth factor antibody, has been used for the treatment of radiation necrosis. Thus far, however, there has been no definitive report on its use for the treatment of symptomatic pseudoprogression. Here we report 2 cases of successful treatment with bevacizumab for symptomatic pseudoprogression after boron neutron capture therapy (BNCT) was applied for recurrent malignant gliomas.
Methods. Two recurrent malignant gliomas received BNCT. Both cases were treated with intravenous administration of bevacizumab at the deterioration that seemed to be symptomatic pseudoprogression.
Results. The first case was recurrent glioblastoma multiforme and the second was recurrent anaplastic oligoastrocytoma. Both cases recurred after standard chemoradiotherapy and were referred to our institute for BNCT, which is tumor-selective particle radiation. Just prior to neutron irradiation, PET with an amino acid tracer was applied in each case to confirm tumor recurrence. Both cases showed deterioration in symptoms, as well as on MRI, at intervals of 4 months and 2 months, respectively, after BNCT. For the first case, a second PET was applied in order to confirm no increase in tracer uptake. We diagnosed both cases as symptomatic pseudoprogression and started the intravenous administration of 5 mg/kg bevacizumab biweekly with 6 cycles. Both cases responded well to this, showing rapid and dramatic improvement in neuroimaging and clinical symptoms. No tumor progression was observed 8 months after BNCT.
Conclusions. Bevacizumab showed marked effects on symptomatic pseudoprogression after BNCT. BNCT combined with bevacizumab may prolong the survival of patients with recurrent malignant gliomas.

Keywords: bevacizumab, boron neutron capture therapy, malignant gliomas, pseudoprogression.

With the advent of temozolomide (TMZ), concomitant chemoradiation and maintenance chemotherapy with TMZ have become the worldwide standard treatment for malignant gliomas (MGs), especially glioblastoma multiforme (GBM).[1] In GBM treatments, pseudoprogression (psPD) can be encountered with a relatively high frequency, especially in O^6-DNA methylguanine-methyltransferase (MGMT) promoter methylated cases,[2] and intensive treatment might be the primary factor in psPD, as Brandsma et al reported.[3] Boron neutron capture therapy (BNCT) is biochemically targeted radiation based on the nuclear capture and fission reactions that occur when nonradioactive boron-10, which is a constituent of natural elemental boron, is irradiated with low-energy thermal neutrons to yield high linear energy transfer alpha particles and recoiling lithium-7 nuclei. Because these particles are released within a very short range, such as 9 μm, the cytotoxic effects are confined within boron-10–containing cells.[4] Boron-10–containing compounds can be accumulated selectively into tumor cells by several mechanisms. For example,

Received October 8, 2012; accepted January 25, 2013.

Corresponding Author: Shin-Ichi Miyatake, MD, PhD, Department of Neurosurgery, Osaka Medical College, 2-7 Daigaku-machi, Takatsuki City, Osaka 569-8686, Japan (neu070@poh.osaka-med.ac.jp).

boronophenylalanine (BPA) is selectively and preferentially accumulated into tumor cells via the augmented metabolism of amino acids in comparison with normal cells. We applied BNCT aggressively to newly diagnosed and recurrent MGs.[5–7] We previously reported a high incidence of psPD after BNCT, not only in MGs but also in malignant meningiomas.[8] However, it is difficult for us to estimate precisely the psPD occurrence rate after BNCT, because many cases were followed up after BNCT by physicians in charge in many towns in Japan. Nevertheless, we have the impression that psPD might occur more frequently by BNCT than by X-ray treatment and that the rate of psPD after BNCT might be higher in recurrent cases than in newly diagnosed cases.

Bevacizumab, an anti–vascular endothelial growth factor (VEGF) antibody, has been used for the treatment of symptomatic radiation necrosis (RN).[9,10] It is difficult to definitively distinguish RN from psPD. We therefore applied intravenous administration of bevacizumab to cases we highly suspected to be symptomatic psPD encountered after BNCT for recurrent MGs. Here we report 2 successfully treated cases of symptomatic psPD after BNCT with bevacizumab.

Case Presentation

Case 1

A 56-year-old male experienced speech disturbance and consequently retired from his job. First he received a craniotomy in April 2008 with a diagnosis of gemistocytic astrocytoma followed by fractionated X-ray treatment (total 50 Gy) and repetitive chemotherapy with nitrosourea. In April 2011, a recurrent lesion appeared with gadolinium (Gd) enhancement on MRI. Re-craniotomy revealed GBM histologically. After surgery, the enhanced lesion gradually grew, and sensory aphasia was aggravated despite the repeated administration of TMZ. Also, carbon 11–labeled methionine PET (C-Met-PET) showed high uptake of the tracer beyond the Gd-enhanced lesion. The patient was then referred to our institute for BNCT. Upon referral, MRI showed a small ringlike enhanced lesion having satellite-enhanced dots in the left temporal lobe, with a relatively large volume of fluid-attenuated inversion recovery (FLAIR) at high intensity, as shown in Fig. 1A and D. A simultaneous fluorine 18–labeled (F)-BPA-PET image showed marked tracer uptake in the left temporo-parietal region, as shown in Fig. 2A, with a 5.5 lesion/normal (L/N) brain ratio of the tracer, indicating that the lesion was a highly malignant tumor.

We administered BNCT to our patient according to our recent protocol for recurrent MGs and malignant meningiomas. Briefly, only BPA was administered in the 2 h (200 mg/kg/h) just prior to neutron irradiation and then during neutron irradiation (100 mg/kg/h). The irradiation time was decided by simulation not to exceed 12.0 Gy-Eq (Gray-equivalent) for the peak brain dose. Using BNCT, we estimated maximum brain dose, maximum tumor dose, and minimum tumor dose as 10.8, 110, and 82.3 Gy-Eq, respectively. Here, Gy-Eq corresponds to the biologically equivalent X-ray dose that would have equivalent effects on

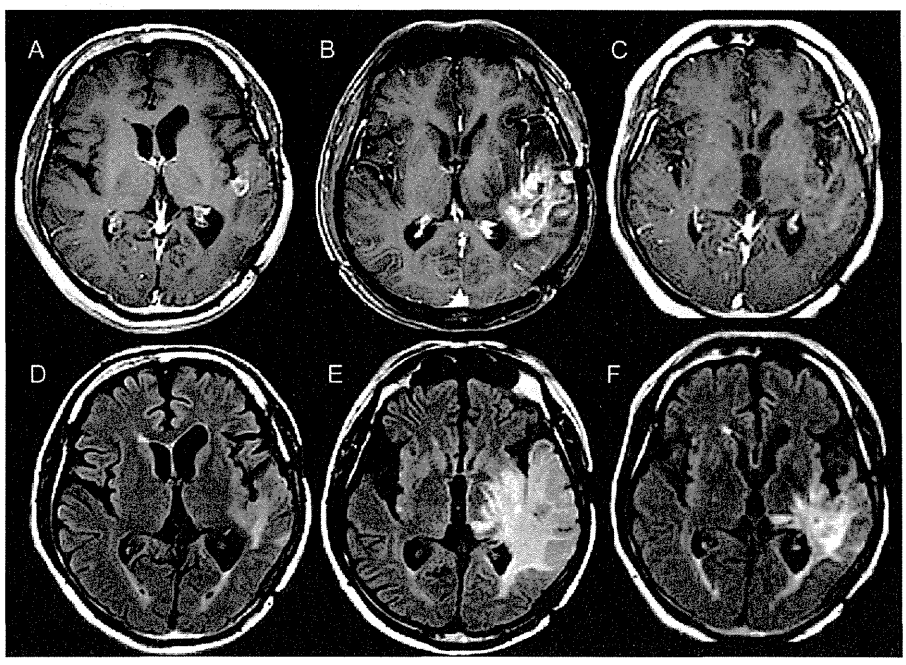

Fig. 1. Periodic MRI changes in case 1. (A–C) Gd-enhanced T1-weighted MRI. (D–F) FLAIR MRI. (A and D) Just prior to BNCT; (B and E) 4 months after BNCT; (C and F) 7 months after BNCT (3 cycles after initial bevacizumab treatment).

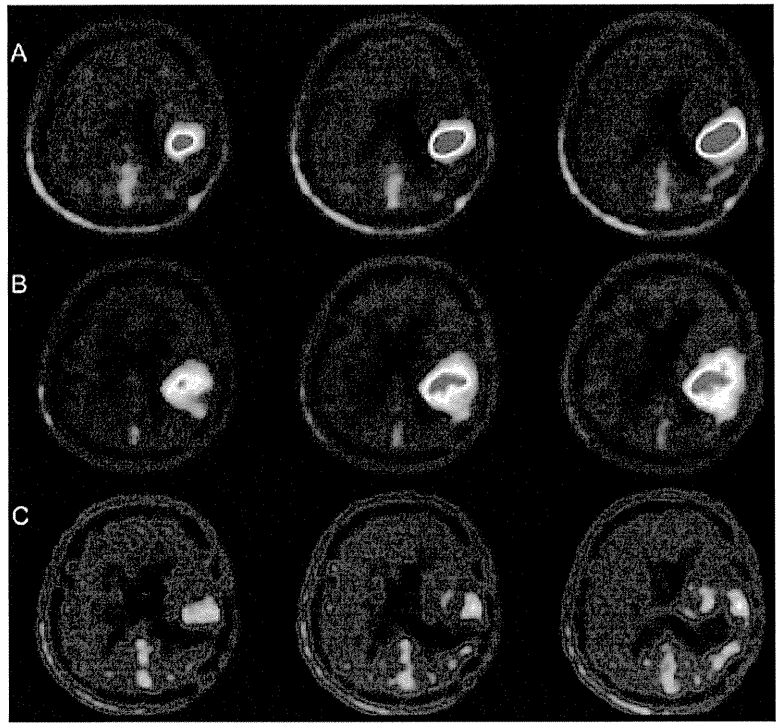

Fig. 2. F-BPA-PET in case 1, prior to BNCT and at aggravation as well as in follow-up with the patient in good condition. (A) Prior to BNCT; (B) 4 months after BNCT (at aggravation); (C) 8 months after BNCT.

tumors and on the normal brain. The dose estimation method was described previously.[8]

One week after BNCT, anticoagulant and vitamin E were administered. This was for the prevention of RN, as we reported previously.[9] Right hemiparesis and aphasia occurred and became aggravated gradually after BNCT, even with an escalated dose of corticosteroids. Then, 4 months after BNCT, follow-up MRI and F-BPA-PET were applied simultaneously. In MRI, the Gd-enhanced lesion and the high-intensity area in FLAIR increased markedly (Fig. 1B and E). The second F-BPA-PET, taken 4 months after BNCT, showed decreased uptake of the tracer, as shown in Fig. 2B (L/N ratio, 4.7). Thereafter, the aggravation of clinical symptoms and MRIs was attributed not to tumor progression but to psPD.

We proposed bevacizumab treatment to the patient, his family, and the physician in charge. Thereafter, he was administered 5 mg/kg bevacizumab biweekly with 6 cycles. MRI taken after 3 cycles showed marked improvement in both Gd-enhanced and FLAIR images, as shown in Fig. 1C and F. The patient's speech disturbance and hemiparesis improved markedly by the treatment. The third F-BPA-PET, undertaken 8 months after BNCT with the patient in a stable state, showed a further decrease of tracer uptake, with an L/N ratio of 1.8, as shown in Fig. 2C. This finding suggests no tumor progression and good control of the tumor so far. The follow-up MRI showed no tumor progression (data not shown).

Case 2

A 27-year-old female developed left hemiparesis. A right frontal enhanced mass was removed gross totally in May 2005. The histological diagnosis was anaplastic oligoastrocytoma. She received fractionated X-ray treatment (total 72 Gy) and repetitive chemotherapy with nitrosourea. The lesion recurred and re-craniotomy was applied in November 2009 with the same pathological diagnosis. This was followed by successive TMZ chemotherapy. Unfortunately, the recurrence was confirmed by MRI and C-Met-PET, and the patient retired from her job as a nurse due to progression of left hemiparesis and seizures. She was referred to us for BNCT. Upon referral, MRI showed a Gd-enhanced lesion in the right frontal lobe with moderate perifocal edema, as shown in Fig. 3A and D.

For this case, BNCT was applied using the same protocol described in case 1. In BNCT, the maximum brain dose, maximum tumor dose, and minimum tumor dose were 11.5, 71.6, and 30.1 Gy-Eq, respectively. In this case, anticoagulant and vitamin E were also administered 1 week after BNCT to prevent RN. After BNCT, her hemiparesis became aggravated gradually even with an increasing dose of corticosteroids. MRI taken 2 months after BNCT showed an enlarged enhanced lesion with increased perilesional edema (Fig. 3B and E). The patient had no chance to receive further amino acid PET, but we considered this aggravation as symptomatic of psPD based on the duration of aggravation after

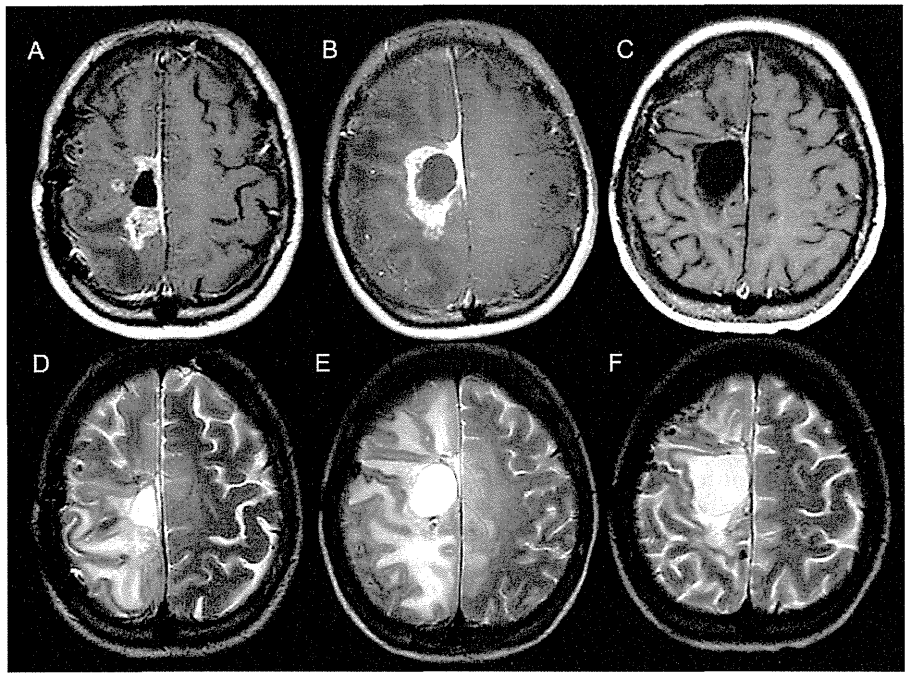

Fig. 3. Periodic MRI changes in case 2. (A–C) Gd-enhanced T1-weighted MRI. (D–F) T2-weighted MRI. (A and D) Just prior to BNCT; (B and E) 2 months after BNCT; (C and F) 6 months after BNCT (4 cycles after initial bevacizumab treatment).

BNCT. This patient and her physician in charge also accepted our proposal of bevacizumab treatment on the same schedule and dosage described in case 1. The patient was bed-ridden just prior to bevacizumab treatment, but her hemiparesis improved markedly and she could walk after 2 cycles of the treatment. MRI taken after 4 cycles, at 6 months after BNCT, showed marked improvement not only in Gd enhancement but also in the perilesional edema in FLAIR images, as shown in Fig. 3C and F. Her clinical condition has remained stable and good since the treatment ended.

Discussion

In our limited experience, there is no obvious histological difference between RN and psPD.[8,11] Necrosis is the central histopathological feature of each, and prominent angiogenesis is common at the boundary of central necrosis and normal brain tissue in each clinicopathological entity. Clinically, psPD usually occurs at a relatively early stage after some intensive treatments and is self-limiting. In most cases it improves over time without intensive treatments. On the other hand, RN often shows severe symptoms and occurs at least 6 months after radiotherapy. It is often long-lasting and improves only with intensive treatment, such as lesionectomy or bevacizumab administration. In human surgical specimens of RN, we previously demonstrated that overproduction of VEGF in reactive astrocytes in the perinecrotic area caused leaky angiogenesis, and this is the cause of perifocal edema in RN.[10] So we speculated that bevacizumab might neutralize this overproduced VEGF in the perinecrotic area and subsequently reduce the edema.[10] This is why we used bevacizumab for symptomatic psPD.

Originally, F-BPA-PET was developed for the simulation of absorbed dose in BNCT.[6,12,13] On the other hand, the background uptake of the tracer F-BPA is very low compared with that of fluorodeoxyglucose and even with that of methionine as a tracer. Thereafter, RN and psPD have been differentially diagnosed from tumor progression by F-BPA-PET.[8,14] On the basis of our experience, an L/N ratio of <2.0 in F-BPA-PET indicates a high possibility of RN and does not indicate tumor progression. We are now performing a nationwide multicenter clinical trial of bevacizumab treatment for symptomatic RN in the brain with diagnosis made by amino acid tracer PET. F-BPA-PET and C-Met-PET are equally useful for the differential diagnosis between RN and tumor progression. Both PETs show the same tendencies of tracer uptake and distribution, as Nariai et al reported.[15]

Both cases presented here were recurrent MGs and had received fractionated X-ray treatment previously. They showed aggravated clinical symptoms and MRI results a couple of months after BNCT. Therefore, we considered both cases to be symptomatic psPD. Especially in case 1, repetitive F-BPA-PETs were applied before BNCT and upon aggravation after BNCT, as well as in a stable state during follow-up. The second F-BPA-PET showed a lower L/N ratio than the first, but it was still higher than our criterion for RN at the aggravation. This may suggest that the

pathology of case 1 was psPD and not RN. Although the essential difference between them is still unclear, we speculated that they may have similar pathophysiology.

Usually we can treat asymptomatic psPD only with corticosteroids, or we can only observe the patient in asymptomatic psPD without treatments. Unfortunately, both cases presented here continued their clinical deterioration despite the escalating doses of corticosteroids. Fortunately, however, we used bevacizumab thereafter, to which both cases responded well. The physicians in charge decreased the corticosteroid dose for each patient after bevacizumab treatment.

To improve the effectiveness of radiotherapy, one study used bevacizumab with hypofractionated stereotactic irradiation for the treatment of recurrent MGs.[16] However, the literature contains no obvious reports about bevacizumab's effects on symptomatic psPD. We applied bevacizumab treatment to symptomatic RN in some cases, and all the patients responded well.[9] Based on these findings, as noted, we are performing a nationwide multicenter clinical trial of bevacizumab treatment for symptomatic RN in the brain. We therefore treated the present 2 cases with bevacizumab and confirmed marked effects. Some of the literature supports this concept.[17]

We applied BNCT, a tumor-selective particle radiation, aggressively even for recurrent MGs with satisfactory results, as reported elsewhere.[7] In that previous report, we used Carson et al[18] as our reference regarding BNCT's effectiveness for recurrent MGs; those authors advocated, and we adopted, recursive portioning analysis (RPA) classification for recurrent MGs. In our previous report,[7] we showed good effectiveness, especially in poor prognosis groups (RPA classes 3 and 7[18]) in BNCT in comparison with Carson's original data sets. Those authors reported that RPA classes 3 and 7 showed the poorest prognosis, with median survival times (MSTs) of 3.8 months and 4.9 months, respectively, after recurrence that followed some treatments. Both of the cases presented here should be considered RPA class 3 because they showed poor performance status at recurrence and because the initial histological diagnosis was not GBM. Carson's data sets revealed an MST of 3.8 months in RPA class 3 after recurrence. Both cases presented here survived more than 8 months after BNCT without tumor progression, continuing up to the writing of this manuscript. Although the 2 cases reported here are the only 2 that we have experienced with symptomatic psPD treated by bevacizumab after BNCT, BNCT plus bevacizumab at psPD improves a patient's condition and may prolong survival more effectively for recurrent MGs than we suggested in our previous report.

Bevacizumab treatment had no adverse effect in either of the present cases. As we described for each case, we routinely used anticoagulant after BNCT for recurrent MGs. This was to prevent anticipated RN. This anticoagulant administration probably decreases the possible adverse effects of thromboembolitic complications of bevacizumab, as we and Levin et al have reported.[9,10]

As noted at the beginning of this paper, it is widely accepted that MGMT promoter methylation status plays a significant role in the incidence of psPD in newly diagnosed GBM cases treated by concomitant chemo therapy and radiation.[2] So let us add finally some information regarding MGMT in both cases presented here. In case 1, MGMT protein expression was positive in immunohistochemistry, and in case 2, the MGMT promoter was methylated. These observations might suggest that MGMT status is not so important for the incidence of symptomatic psPD for recurrent MGs receiving BNCT.

Funding

This work was supported in part by Grants-in-Aid for Scientific Research (B) (19390385) from the Japanese Ministry of Education, Culture, Sports, Science, and Technology to S.-I. M.

Conflict of interest statement. None declared.

References

1. Stupp R, Mason WP, van den Bent MJ, et al. Radiotherapy plus concomitant and adjuvant temozolomide for glioblastoma. *N Engl J Med*. 2005;352:987–996.
2. Brandes AA, Franceschi E, Tosoni A, et al. MGMT promoter methylation status can predict the incidence and outcome of pseudoprogression after concomitant radiochemotherapy in newly diagnosed glioblastoma patients. *J Clin Oncol*. 2008;26:2192–2197.
3. Brandsma D, Stalpers L, Taal W, Sminia P, van den Bent MJ. Clinical features, mechanisms, and management of pseudoprogression in malignant gliomas. *Lancet Oncol*. 2008;9:453–461.
4. Barth RF, Vicente MG, Harling OK, et al. Current status of boron neutron capture therapy of high grade gliomas and recurrent head and neck cancer. *Radiat Oncol*. 2012;7:146.
5. Kawabata S, Miyatake S, Kuroiwa T, et al. Boron neutron capture therapy for newly diagnosed glioblastoma. *J Radiat Res (Tokyo)*. 2009;50:51–60.
6. Miyatake S, Kawabata S, Kajimoto Y, et al. Modified boron neutron capture therapy for malignant gliomas performed using epithermal neutron and two boron compounds with different accumulation mechanisms: an efficacy study based on findings on neuroimages. *J Neurosurg*. 2005;103:1000–1009.
7. Miyatake S, Kawabata S, Yokoyama K, et al. Survival benefit of boron neutron capture therapy for recurrent malignant gliomas. *J Neurooncol*. 2009;91:199–206.
8. Miyatake S, Kawabata S, Nonoguchi N, et al. Pseudoprogression in boron neutron capture therapy for malignant gliomas and meningiomas. *Neuro Oncol*. 2009;11:430–436.
9. Furuse M, Kawabata S, Kuroiwa T, Miyatake S. Repeated treatments with bevacizumab for recurrent radiation necrosis in patients with malignant brain tumors: a report of 2 cases. *J Neurooncol*. 2011;102:471–475.

10. Levin VA, Bidaut L, Hou P, et al. Randomized double-blind placebo-controlled trial of bevacizumab therapy for radiation necrosis of the central nervous system. *Int J Radiat Oncol Biol Phys*. 2011;79:1487–1495.
11. Nonoguchi N, Miyatake S, Fukumoto M, et al. The distribution of vascular endothelial growth factor–producing cells in clinical radiation necrosis of the brain: pathological consideration of their potential roles. *J Neurooncol*. 2011;105:423–431.
12. Imahori Y, Ueda S, Ohmori Y, et al. Positron emission tomography–based boron neutron capture therapy using boronophenylalanine for high-grade gliomas: part I. *Clin Cancer Res*. 1998;4:1825–1832.
13. Imahori Y, Ueda S, Ohmori Y, et al. Positron emission tomography–based boron neutron capture therapy using boronophenylalanine for high-grade gliomas: part II. *Clin Cancer Res*. 1998;4:1833–1841.
14. Miyashita M, Miyatake S, Imahori Y, et al. Evaluation of fluoride-labeled boronophenylalanine-PET imaging for the study of radiation effects in patients with glioblastomas. *J Neurooncol*. 2008;89:239–246.
15. Nariai T, Ishiwata K, Kimura Y, et al. PET pharmacokinetic analysis to estimate boron concentration in tumor and brain as a guide to plan BNCT for malignant cerebral glioma. *Appl Radiat Isot*. 2009;67:S348–S350.
16. Gutin PH, Iwamoto FM, Beal K, et al. Safety and efficacy of bevacizumab with hypofractionated stereotactic irradiation for recurrent malignant gliomas. *Int J Radiat Oncol Biol Phys*. 2009;75:156–163.
17. Khasraw M, Simeonovic M, Grommes C. Bevacizumab for the treatment of high-grade glioma. *Expert Opin Biol Ther*. 2012;12:1101–1111.
18. Carson KA, Grossman SA, Fisher JD, Shaw EG. Prognostic factors for survival in adult patients with recurrent glioma enrolled onto the new approaches to brain tumor therapy CNS consortium phase I and II clinical trials. *J Clin Oncol*. 2007;25:2601–2606.

Japanese Journal of Clinical Oncology Advance Access published January 8, 2013

JJCO Japanese Journal of Clinical Oncology

Jpn J Clin Oncol 2013
doi:10.1093/jjco/hys231

Short Communication

Bevacizumab Treatment for Symptomatic Radiation Necrosis Diagnosed by Amino Acid PET

Motomasa Furuse[1,*], Naosuke Nonoguchi[1], Shinji Kawabata[1], Erina Yoritsune[1], Masatsugu Takahashi[2], Taisuke Inomata[2], Toshihiko Kuroiwa[1] and Shin-Ichi Miyatake[1]

[1]Department of Neurosurgery, Osaka Medical College and [2]Department of Radiology, Osaka Medical College, Takatsuki, Osaka, Japan

*For reprints and all correspondence: Motomasa Furuse, Department of Neurosurgery, Osaka Medical College, 2-7, Daigakumachi, Takatsuki, Osaka 569-8686, Japan. E-mail: neu054@poh.osaka-med.ac.jp

Received September 4, 2012; accepted December 12, 2012

Bevacizumab is effective in treating radiation necrosis; however, radiation necrosis was not definitively diagnosed in most previous reports. Here we used amino acid positron emission tomography to diagnose radiation necrosis for the application of bevacizumab in treating progressive radiation necrosis. Lesion/normal tissue ratios of <2.5 on ^{18}fluoride-labeled boronophenylalanine-positron emission tomography were defined as an indication of effective bevacizumab treatment. Thirteen patients were treated with bevacizumab at a dose of 5 mg/kg every 2 weeks. Two patients were excluded because of adverse events. The median reduction rate in perilesional edema was 65.5%. Karnofsky performance status improved in six patients after bevacizumab treatment. Lesion/normal tissue ratios on ^{18}fluoride-labeled boronophenylalanine-positron emission tomography ($P = 0.0084$) and improvement in Karnofsky performance status after bevacizumab treatment ($P = 0.0228$) were significantly associated with reduced rates of perilesional edema. Thus, ^{18}fluoride-labeled boronophenylalanine-positron emission tomography could be useful for diagnosing radiation necrosis and predicting the efficacy of bevacizumab in progressive radiation necrosis.

Key words: bevacizumab – brain edema – Karnofsky performance status – positron emission tomography – radiation necrosis

INTRODUCTION

Radiation necrosis, a well-known late adverse effect of radiotherapy, is an intractable iatrogenic disease. Symptomatic radiation necrosis negatively affects the patient's quality of life and can cause harmful lifelong effects, despite the possible positive effects on life span that intensive radiotherapy can provide. Recently, bevacizumab has been shown to dramatically decrease focal edema around the necrotic core, and thus, be an effective treatment for symptomatic radiation necrosis (1–4). With this discovery, the outlook for radiation necrosis has become hopeful, but accurate diagnosis of radiation necrosis remains problematic. Radiation necrosis was not definitively diagnosed in most reports to date, and some patients were diagnosed by magnetic resonance (MR) images alone. Differentiating tumor recurrence or progression from radiation necrosis remains difficult when the enhanced lesion and/or perilesional edema are enlarged on follow-up MR images, even if the tissue is surgically resected for histopathological examination. Positron emission tomography (PET) using an amino acid tracer is among the most promising modalities for the non-invasive diagnosis of radiation necrosis that causes radiographical worsening on MR images. We previously reported that differentiation between tumor progression and radiation necrosis can be achieved with ^{18}fluoride-labeled boronophenylalanine-PET (F-BPA)-PET (5). In the present study, we report the use of bevacizumab to treat patients with progressive radiation necrosis at our institution. Instead of using surgical biopsy, we diagnosed radiation necrosis in these patients based on a

review of MR images and clinical courses and by reference to our cut-off index for ^{18}F-BPA-PET. Our final goal is to establish a non-invasive and effective method of managing radiation necrosis from diagnosis to therapy.

PATIENTS AND METHODS

Patients

The protocol of this study was approved by our institutional review board. Between January 2009 and October 2010, 13 patients with symptomatic radiation necrosis were treated with bevacizumab at our institute. Radiation necrosis was defined as an enhanced lesion that grew slowly, accompanied by the massive perilesional edema on follow-up MR images. All patients underwent ^{18}F-BPA-PET and various first-line medical treatments, including the treatment with corticosteroids, anticoagulants and vitamin E, but had been refractory to these medications. Other inclusion criteria were as follows: $\geq$3 months elapsed after the initial radiotherapy; unresectable lesions; no systemically active lesion and life expectancy $\geq$3 months.

^{18}F-BPA-PET imaging

All ^{18}F-BPA-PET scans were performed at the Nishijin Hospital, Kyoto, Japan. BPA was originally synthesized as described previously (6,7), and the protocol for the PET measurements using a HEADTOME III (Shimadzu Co., Kyoto, Japan) has also been described elsewhere (8,9). Semi-quantitative analysis was performed using the lesion/normal tissue (L/N) ratio. Using Amide software (SourceForge, Inc., Mountain View, CA), regions of interest of 1 cm diameter were placed on the lesion with the maximal uptake of ^{18}F-BPA on PET and on the contralateral brain area. L/N ratios were generated by dividing the mean standardized uptake value (SUV) of the lesion by the mean SUV of the contralateral normal brain. We previously reported that an L/N ratio measured by ^{18}F-BPA-PET of $<$2.0 is indicative of radiation necrosis in patients with glioblastoma treated with radiation therapy (5). An L/N ratio $>$2.5 is strongly suggestive of tumor progression. Therefore, with regard to ^{18}F-BPA-PET, the L/N ratios of equal to or $<$2.0 were an absolute indication for bevacizumab treatment in the present study. Patients with an L/N ratio between 2.0 and 2.5 were also included, provided they had undergone ^{18}F-BPA-PET before tumor treatment and their current L/N ratio was lower than the previous value.

Bevacizumab treatment

Patients were treated with bevacizumab at a dose of 5 mg/kg every 2 weeks. Neurological status and MR images were evaluated after three cycles of bevacizumab treatment. Patients underwent three more cycles of bevacizumab treatment when any clinical or radiological response was obtained after the initial three cycles.

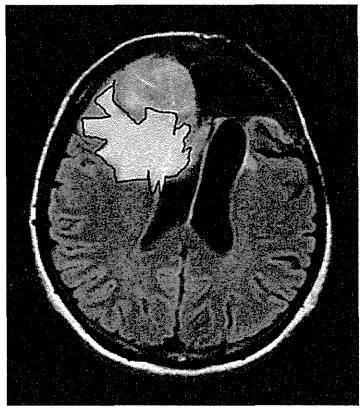

Figure 1. The area of hyperintensity was manually outlined on each FLAIR MR image (black line).

Data analysis

The volume of the hyperintense area on FLAIR MR images before and after bevacizumab treatment was measured in each case using ImageJ software (National Institutes of Health, Bethesda, MD, USA). On each axial MR slice, the area of hyperintensity was manually outlined (Fig. 1), measured and summed across slices. These sums were multiplied by the slice interval. The reduction rate of perilesional edema was calculated by dividing the post-treatment volume by the pretreatment volume. The outcomes were based on MR images, ^{18}F-BPA-PET and histopathological examination. Univariate analyses were conducted using analysis of variance.

RESULTS

Of the 13 patients, 2 were excluded from the analysis because of discontinuation of bevacizumab in response to adverse events. One patient exhibited an asymptomatic intracerebral hemorrhage after one dose of bevacizumab. Periodic MR images revealed this hemorrhage in an area of radiation necrosis without clinical aggravation. Another patient suffered a sudden cardiopulmonary arrest after marked clinical improvements had been observed following two doses of bevacizumab. This patient had a poor Karnofsky performance status (KPS) (KPS 20) and was bedridden prior to treatment. The cause of the cardiopulmonary arrest was not clear. Thus, a total of 11 patients were included in this analysis.

The demographics of the patients are listed in Table 1. The median duration between the final radiotherapy and the start of bevacizumab treatment was 11 months. The median L/N ratio on ^{18}F-BPA-PET was 1.8. The median volumes of perilesional edema before and after bevacizumab treatment were 65.0 and 23.6 cm^3, respectively. The median reduction ratio was 65.5%. KPS improved in six patients after bevacizumab treatment and did not change in five patients. Regarding original tumor pathology, the patients with metastatic brain tumors (Cases 2, 5 and 6) had a good treatment

Table 1. Patients' demographics

Case	Age	Gender	Primary tumors	Location	Size (cm)	Radiotherapies	Duration (months)	Cycles	L/N ratio	Perilesional edema		Reduction rate (%)	Pre-KPS	Post-KPS	T or N PFS (months)
										Pre-Tx (cm^3)	Post-Tx (cm^3)				
1	39	M	GBM	Parietal	6.1	BNCT, XRT	11	6	1.7	43.7	8.3	81.0	90	100	8.5
2	57	F	Met	Frontal	2.2	SRS x2	5	6	1.8	65.0	17.3	73.4	40	60	6.4
3	50	F	GBM	Parietal	6.0	Proton, XRT	37	5	1.6	151.0	77.9	48.4	60	70	15.6
4	55	F	AM	Parietal parasagittal	2.6	XRT, SRS, BNCT	6	6	2.2	31.8	25.7	19.4	60	60	13.8
5	74	F	Met	Frontal	2.3	SRS	47	6	1.5	12.9	3.3	74.4	60	60	11.5
6	55	M	Met	Frontal	1.5	SRS	49	6	2.0	101.0	22.8	77.5	80	90	10.3
7	38	M	GBMO	Frontal	3.2	XRT	6	4	1.8	133.0	37.4	71.9	60	70	12.7
8	27	F	AA	Frontal	4.6	BNCT, XRT	44	3	1.6	75.3	25.9	65.5	90	100	17.5
9	65	M	GBM	Frontal	6.0	XRT	11	3	2.2	95.8	93.9	2.0	40	40	1.3
10	76	M	AM	Frontal parasagittal	4.6	SRS x2, SRT x2	6	3	2.2	29.7	23.6	20.5	60	60	8.0
11	35	M	AM	Falco-tentorial	4.7	XRT, SRS	7	3	1.8	48.4	22.3	54.0	60	60	2.2

AA, anaplastic astrocytoma; AM, anaplastic meningioma; BNCT, boron neutron capture therapy; GBM, glioblastoma multiforme; GBMO, glioblastoma multiforme with oligodendroglial component; KPS, Karnofsky performance status; Met, metastatic brain tumor; SRS, stereotactic radiosurgery; SRT, stereotactic radiotherapy; T or N PFS, tumor or necrosis progression-free survival; Tx, treatment; XRT, X-ray radiotherapy.

response (>70% reduction, Fig. 2). The L/N ratio on ^{18}F-BPA-PET ($P = 0.0084$) and the improvement of KPS after bevacizumab treatment ($P = 0.0228$) were significantly associated with the response rate of then perilesional edema after bevacizumab treatment in univariate analysis (Table 2). A case is illustrated in Fig. 3.

During the median follow-up period of 14.4 months (range, 2.9–32.4), two patients were stable, radiation necrosis recurred in two patients and the tumor progressed or a new tumor lesion appeared in seven patients. The 6-month and 1-year tumor-progression-free survival rates from the PET study were 90.9 and 63.6%, respectively. The 6-month and 1-year tumor or necrosis progression-free survival rates after bevacizumab treatment were 81.8 and 36.4%, respectively.

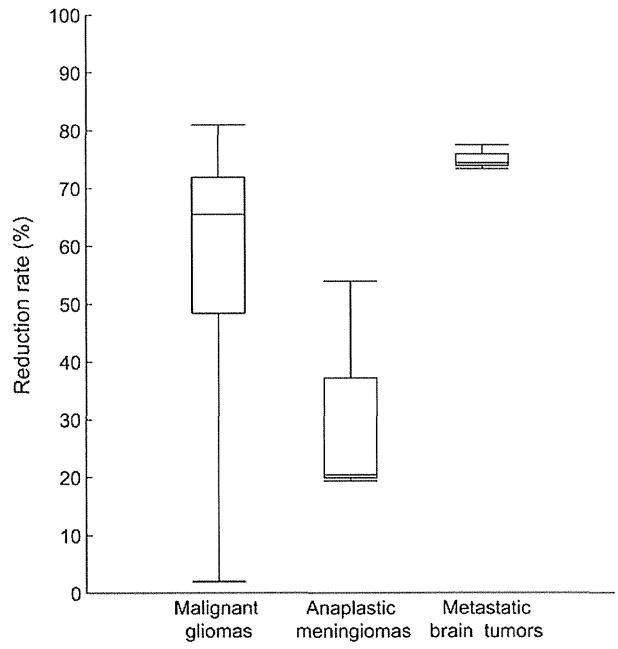

Figure 2. Box plots demonstrating reduction rates of perilesional edema in each tumor pathology.

DISCUSSION

Radiation necrosis has been treated with bevacizumab in an exploratory fashion and several papers have already reported its clinical effectiveness (1–4). In an animal model of radiation injury, hypoxia induces the vascular endothelial growth factor (VEGF) expression in reactive astrocytes (10). We also demonstrated that VEGF is involved in angiogenesis near the center of radiation necrosis in humans (11). In the present study, there were only two clinical factors, improvement of KPS and L/N ratios on ^{18}F-BPA-PET, which were significantly associated with the response rate of perilesional edema after bevacizumab treatment. Specifically, the reduction in perilesional edema contributed to the improvement in KPS after bevacizumab treatment. Although bevacizumab cannot induce functional recovery of necrotic tissue

Table 2. Regression analysis of clinical factors affecting the reduction rate of perilesional edema

	P value
Age	0.1990
Gender	0.7785
Primary tumor	
Malignant gliomas	0.9753
Metastatic brain tumors	0.1131
Malignant meningiomas	0.1053
Radiotherapy	
X-ray radiotherapy	0.4957
Stereotactic radiosurgery	0.9753
Times of radiation therapies	0.2460
Duration of bevacizumab	0.2293
Cycles of bevacizumab	0.1492
L/N ratio on ^{18}F-BPA-PET	0.0084*
Pretreatment of perilesional edema	0.8426
Pretreatment of KPS	0.1222
Improvement in KPS	0.0228*

*P values of <0.05 were considered statistically significant.

per se, the improvement in perilesional edema around the necrotic core is clinically beneficial for patients with symptomatic radiation necrosis. High-dose radiation therapies and repeated radiotherapies prolong patient survival, but they inevitably increase the incidence of radiation necrosis. Therefore, bevacizumab is expected to produce further beneficial effects of high-dose radiation therapies or repeated radiotherapies in the treatment of central nervous system malignancies. However, it cannot be overlooked that 2 of the 13 patients in the present study experienced adverse events, although it is unknown whether these events were due to bevacizumab.

^{18}F-BPA is an amino acid tracer similar to ^{11}carbon (C)-labeled methionine. Initially, we used this type of PET to determine when BNCT was indicated for treatment of malignant gliomas (12). However, we recently used ^{18}F-BPA-PET to assist with the preliminary evaluation of biological tumor (lesion) activity, and we reported that there were significant differences between histologically proven tumor progression and radiation necrosis in L/N ratios observed on ^{18}F-BPA-PET imaging in patients with glioblastoma (5,13). ^{11}C-methionine PET has also been used to provide quantitative values to aid in the differentiation of tumor recurrence from radiation necrosis in patients with central nervous system malignancies (14). One pharmacokinetic analysis demonstrated that the estimated tumor/

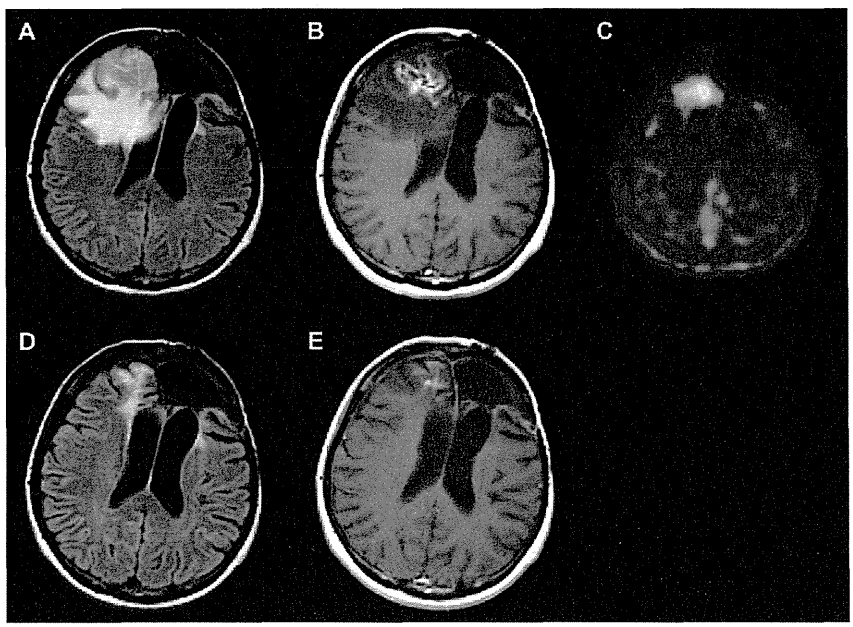

Figure 3. A 27-year-old woman (Case 8) with a left frontal anaplastic astrocytoma was treated with BNCT and X-ray radiotherapy after surgical resection. The patient had a convulsion due to enlarged perilesional edema 4 years later. MR images showed a heterogeneous enhancement with the massive perilesional edema in the right frontal lobe (A, B). The L/N ratio was 1.6 on F-BPA-PET (C). The patient was treated with bevacizumab. MR images after six cycles showed a remarkable reduction in perilesional edema and a weakening of the abnormal enhancement (D, E). The patient did not experience any further convulsions.

normal (T/N) ratio of tissue boron concentration, T/N ratio of ^{18}F-BPA and T/N ratio of ^{11}C-methionine showed significant linear correlations among each other in glioma patients (15). Pathological heterogeneity is the main reason for difficulty in distinguishing between tumor progression and radiation necrosis. Even if PET analysis suggests that a lesion is radiation necrosis, it does not exclude the possible existence of a few living tumor cells in or around the lesion. In other words, amino acid PET is useful for assessing whether the predominant cause of increasing radiographical enhancement and perilesional edema is tumor progression or radiation necrosis. The 6-month tumor-progression-free survival rates of 90.9% clearly show that ^{18}F-BPA-PET is a reliable tool that can be used to judge the predominant cause of the progressive perilesional edema in patients with brain tumors previously treated with radiotherapy.

In the present study, there was a statistically significant negative correlation between the L/N ratios on ^{18}F-BPA-PET and the reduction rates of perilesional edema. Although it is not easy to interpret the data, we hypothesize that an FLAIR-hyperintense area around a lesion with a high L/N ratio consists of not only vasogenic edema but also tumor invasion to some degree. This hypothesis is supported by the finding that perilesional edema in radiation necrosis with metastatic brain tumors responded much more strongly to bevacizumab treatment than perilesional edema in radiation necrosis with other tumors. Malignant gliomas and malignant meningiomas are presumably more infiltrative than metastatic brain tumors. Malignant gliomas showed varied responses to bevacizumab, and malignant meningiomas generally had low responses to bevacizumab. Cases with malignant meningiomas had long disease durations and underwent multiple radiotherapies before bevacizumab treatment. Therefore, FLAIR hyperintensity around the necrotic core may not indicate purely vasogenic edema in malignant meningiomas. Except for our previous case report (1), there have been no reports on the use of bevacizumab in the treatment of radiation necrosis occurring after radiotherapy for metastatic brain tumors. In the present study, radiation necrosis with metastatic brain tumors homogenously responded to bevacizumab very well, although the study only included three such cases. Bevacizumab treatment in patients with metastatic brain tumors is controversial because the risk of hemorrhagic complication is always a concern. However, Besse et al. recently reported that patients with central nervous system metastasis have a similar risk of developing cerebral hemorrhage independent of bevacizumab therapy (16). Thus, we believe patients with symptomatic radiation necrosis treated for metastatic brain tumors are good candidates for bevacizumab treatment. At present, our larger clinical trial of bevacizumab treatment of symptomatic radiation necrosis including patients with metastatic brain tumors treated with radiotherapy is ongoing under the system of investigational medical care approved by the Ministry of Health, Labour and Welfare.

Funding

This work was supported by a JSPS Grant-in-Aid for Scientific Research (C) (Grant Number: 23592145).

Conflict of interest statement

None declared

References

1. Furuse M, Kawabata S, Kuroiwa T, Miyatake SI. Repeated treatments with bevacizumab for recurrent radiation necrosis in patients with malignant brain tumors: a report of 2 cases. *J Neurooncol* 2011;102:471–5.
2. Gonzalez J, Kumar AJ, Conrad CA, Levin VA. Effect of bevacizumab on radiation necrosis of the brain. *Int J Radiat Oncol Biol Phys* 2007;67:323–6.
3. Levin VA, Bidaut L, Hou P, et al. Randomized double-blind placebo-controlled trial of bevacizumab therapy for radiation necrosis of the central nervous system. *Int J Radiat Oncol Biol Phys* 2011;79:1487–95.
4. Torcuator R, Zuniga R, Mohan YS, et al. Initial experience with bevacizumab treatment for biopsy confirmed cerebral radiation necrosis. *J Neurooncol* 2009;94:423–31.
5. Miyashita M, Miyatake S, Imahori Y, et al. Evaluation of fluoride-labeled boronophenylalanine-PET imaging for the study of radiation effects in patients with glioblastomas. *J Neurooncol* 2008;89:239–46.
6. Ishiwata K, Ido T, Mejia AA, Ichihashi M, Mishima Y. Synthesis and radiation dosimetry of 4-borono-2-[18F]fluoro-D,L-phenylalanine: a target compound for PET and boron neutron capture therapy. *Int J Rad Appl Instrum* 1991;42:325–8.
7. Mishima Y, Imahori Y, Honda C, et al. In vivo diagnosis of human malignant melanoma with positron emission tomography using specific melanoma-seeking 18F-DOPA analogue. *J Neurooncol* 1997;33:163–9.
8. Imahori Y, Ueda S, Ohmori Y, et al. Fluorine-18-labeled fluoroboronophenylalanine PET in patients with glioma. *J Nucl Med* 1998;39:325–33.
9. Takahashi Y, Imahori Y, Mineura K. Prognostic and therapeutic indicator of fluoroboronophenylalanine positron emission tomography in patients with gliomas. *Clin Cancer Res* 2003;9:5888–95.
10. Li YQ, Ballinger JR, Nordal RA, Su ZF, Wong CS. Hypoxia in radiation-induced blood-spinal cord barrier breakdown. *Cancer Res* 2001;61:3348–54.
11. Nonoguchi N, Miyatake SI, Fukumoto M, et al. The distribution of vascular endothelial growth factor-producing cells in clinical radiation necrosis of the brain: Pathological consideration of their potential roles. *J Neurooncol* 2011;105:423–31.
12. Miyatake S, Kawabata S, Kajimoto Y, et al. Modified boron neutron capture therapy for malignant gliomas performed using epithermal neutron and two boron compounds with different accumulation mechanisms: an efficacy study based on findings on neuroimages. *J Neurosurg* 2005;103:1000–9.
13. Miyatake SI, Kawabata S, Nonoguchi N, et al. Pseudoprogression in boron neutron capture therapy for malignant gliomas and meningiomas. *Neuro Oncol* 2009;11:430–6.
14. Terakawa Y, Tsuyuguchi N, Iwai Y, et al. Diagnostic accuracy of 11C-methionine PET for differentiation of recurrent brain tumors from radiation necrosis after radiotherapy. *J Nucl Med* 2008;49:694–9.
15. Nariai T, Ishiwata K, Kimura Y, et al. PET pharmacokinetic analysis to estimate boron concentration in tumor and brain as a guide to plan BNCT for malignant cerebral glioma. *Appl Radiat Isot* 2009;67: S348–50.
16. Besse B, Lasserre SF, Compton P, et al. Bevacizumab safety in patients with central nervous system metastases. *Clin Cancer Res* 2010;16:269–78.

J Neurosurg 119:837–844, 2013

Boron neutron capture therapy for recurrent high-grade meningiomas

Clinical article

*Shinji Kawabata, M.D., Ph.D.,[1] Ryo Hiramatsu, M.D., Ph.D.,[1] Toshihiko Kuroiwa, M.D., Ph.D.,[1] Koji Ono, M.D., Ph.D.,[2] and Shin-Ichi Miyatake, M.D., Ph.D.[1]

[1]*Department of Neurosurgery, Osaka Medical College, Takatsuki;* [2]*Radiation Oncology Research Laboratory, Research Reactor Institute, Kyoto University, Kumatori, Osaka, Japan*

Object. Similar to glioblastomas, high-grade meningiomas are difficult pathologies to control. In this study, the authors used boron neutron capture therapy (BNCT), a tumor-selective intensive particle radiation modality, to treat high-grade meningioma.

Methods. From June 2005 to September 2011, BNCT was applied 28 times in 20 cases of recurrent high-grade meningioma. All patients had previously undergone intensive treatments such as repetitive surgeries and multiple sessions of radiation therapy. Fluorine-18–labeled boronophenylalanine (^{18}F-BPA) PET was performed before BNCT in 19 of the 20 cases; BPA is itself a therapeutic compound. Compound uptake, tumor shrinkage, long-term control rate including survival time, and failure pattern of the treated patients were all evaluated.

Results. Eighteen of 19 cases studied using ^{18}F-BPA PET showed good BPA uptake, with ratios of tumor to normal brain greater than 2.7. These ratios indicated the likely effects of BNCT prior to neutron irradiation. The original tumor sizes were between 4.3 cm^3 and 109 cm^3. A mean tumor volume reduction of 64.5% was obtained after BNCT within just 2 months. The median follow-up duration was 13 months. Six patients are still alive; at present, the median survival times after BNCT and diagnosis are 14.1 months (95% CI 8.6–40.4 months) and 45.7 months (95% CI 32.4–70.7 months), respectively. Clinical symptoms before BNCT, such as hemiparesis and facial pain, were improved after BNCT in symptomatic cases. Systemic metastasis, intracranial distant recurrence outside the radiation field, CSF dissemination, and local tumor progression were observed in 6, 7, 3, and 3 cases, respectively, during the clinical course. Apparent pseudoprogression was observed in at least 3 cases. Symptomatic radiation injuries occurred in 6 cases, and were controllable in all but 1 case.

Conclusions. Boron neutron capture therapy may be especially effective in cases of high-grade meningioma. *(http://thejns.org/doi/abs/10.3171/2013.5.JNS122204)*

Key Words • **boron neutron capture therapy** • **boronophenylalanine** • **epithermal neutron** • **high-grade meningioma** • **oncology**

The management of high-grade meningiomas, especially malignant meningiomas, is very difficult. In a large series of patients with this disease, the 5-year recurrence rate of high-grade meningiomas was reported to be 78%–84% and the median survival time was reported to be 6.89 years;[17] in another series, the rate of late mortality due to recurrence after the initial surgery was reported to be 69%.[28] Although some treatments for recurrent high-grade meningioma have been reported, including chemotherapeutic regimens,[4] no standard treatment has yet been established.

For several years now, we have been applying BNCT for recurrent and refractory high-grade meningioma cases shown to be refractory to any intensive treatments currently available.[23,32] Boron neutron capture therapy is a targeted radiation approach that significantly increases the therapeutic ratio compared with that of conventional radiotherapeutic modalities. Boron neutron capture therapy is a binary approach: a boron-10–labeled compound delivers high concentrations of boron-10 to the target tumor, relative to the surrounding normal tissues. This is followed by irradiation with thermal or epithermal neutrons that become thermalized at a certain depth within

Abbreviations used in this paper: ^{18}F-BPA = fluorine-18–labeled BPA; BNCT = boron neutron capture therapy; BPA = boronophenylalanine; BSH = sodium borocaptate; EBRT = external bean radiation therapy; SRS = stereotactic radiosurgery; SRT = stereotactic radiation therapy.

* Drs. Kawabata and Miyatake contributed equally to this work.

the tissues. The short range (5–9 μm) of the α and lithium-7 particles released from the boron-10 (neutron, α) lithium-7 neutron capture reaction makes the microdistribution of boron-10 critically important in therapy.[7] The release of these particles constitutes high linear energy transfer radiation. These characteristics contribute to tumor-selective and strong tumoricidal activity with minimal damage to normal tissue. If sufficient quantities of boron compounds can be made to accumulate selectively in the tumor tissues, BNCT becomes an ideal intensive particle radiotherapy.

The concept of this unique particle radiation therapy with selective uptake of a suitable isotope was first introduced by Locher in 1936.[19] The first clinical trial of BNCT for patients with glioblastoma was reported by Farr et al. in the 1950s.[10] However, the previously used version of BNCT suffered from numerous problems: a lack of neutron penetration, especially for deep-seated tumors; insufficient contrast in boron concentration between tumor and normal tissues; an absolute lack of boron in tumor tissues; and uncertain estimation of the neutron flux captured by the boron-10 atoms in tumor cells. We modified several parts of the procedure to resolve these problems and applied the modified BNCT to the treatment of malignant gliomas.[21] In addition, we reported the effectiveness of BNCT for high-grade meningiomas, with special reference to tumor shrinkage, as a case report and an early case series.[23,32] Now that we have treated 20 patients with high-grade meningioma by BNCT, and observed these patient for more than 1 year, we share further details in this paper, not only about the tumor volume reduction, but also about long-term control rate, including cumulative survival data and treatment failure patterns.

Methods

Patient Population

Twenty patients with recurrent high-grade meningioma were treated with BNCT in the Department of Neurosurgery at Osaka Medical College between June 2005 and September 2011. We report the results from these 20 patients, all of whom were followed up for more than 1 year. The cases consisted of 12 anaplastic, 4 atypical, 2 papillary, and 1 rhabdoid meningioma, and 1 sarcoma that began as an anaplastic meningioma. Patient profiles are detailed in Table 1. All cases were referred to our institute for BNCT due to uncontrolled tumor growth after repetitive surgeries and EBRT or SRS. These patients had already undergone treatment by EBRT alone in 4 cases, by SRS or SRT alone in 13 cases, and by a combination of both in 3 cases.

Fluorine-18–Labeled BPA PET Analysis

The patients underwent ^{18}F-BPA PET to assess the distribution of BPA and to estimate the boron concentration in tumors before neutron irradiation.[15,16,21,23,32] Notably, BPA is itself a therapeutic boron compound. The tumor-to-normal-brain ratio of BPA uptake can be estimated from ^{18}F-BPA PET, and subsequent dose planning is based on this ratio; each ratio of the patients is included in Table 1. The PET study had to be omitted in 1 case of anaplastic meningioma (Case 3) because of machine malfunction.

Clinical Regimen of BNCT for Malignant Meningiomas

This project was approved by the Ethical Committee of Osaka Medical College, and each candidate was also discussed and approved by the board of reviewers at Osaka Medical College and Kyoto University Research Reactor Institute. The clinical regimen of BNCT for malignant meningiomas was modified slightly from that for malignant gliomas.[21] Patients were typically administered 500 mg/kg of BPA with or without 5 or 2.5 g of BSH (Katchem Ltd) per person. Boronophenylalanine was kindly supplied by the Stella Pharma Corporation in the initial cases and afterward was purchased mainly from Interpharma Praha, a.s. As the study period progressed, BSH became difficult to obtain due to its exorbitant cost. Thus, BSH administration was omitted from Cases 7 through 20.

Boronophenylalanine was administered in the 2 hours just prior to neutron irradiation (200 mg/kg/hr) and then during neutron irradiation (100 mg/kg/hr). This administration method was adopted to maintain a steady blood BPA concentration throughout the entire neutron irradiation. When BSH was available, the compound solution was administered for 1 hour, starting at 12 hours prior to neutron irradiation. The boron concentration in the blood was monitored by sampling every 1 to 2 hours after boron compound administration until neutron irradiation was completed. The boron concentrations from BSH in the tumor and brain tissue were assumed to be the same as the blood concentration. The boron concentrations from BPA in the tumor and normal brain were estimated from the tumor-to-normal-brain ratio of ^{18}F-BPA on PET. Judging from the contribution of each boron compound and the relative biological effectiveness of neutron beams and compounds described previously,[24,25] the neutron fluence rate was simulated by the dose-planning system SERA (Simulation Environments for Radiotherapy Applications; Idaho National Engineering and Environmental Laboratory), and the total doses to the tumor and normal brain were estimated. The duration of neutron irradiation was determined not to exceed 15 Gy-Eq to the normal brain. In this instance, Gy-Eq (Gray Equivalent) means an x-ray dose that can provide biologically equivalent effects to total BNCT radiation. After the treatment, the doses given were precisely reestimated.

Assessment of Effectiveness

The effectiveness of this treatment was volumetrically assessed in serial radiographic analysis. The Gd-contrasted lesion on MRI was semiautomatically selected, and the area was measured on each slice based on the contrast cutoff value (increased intensity on MRI by Gd) from the background. The value of the area was calculated as tumor volume by adding the areas of all slices using I-Response software (Cedara Corp.). Based on the diagnostic images before BNCT, the relative values of the tumor volume (percentage of control) were calculated from